Patient characteristics and transplant outcomes

	RIC ($n = 91$)	CIC ($n = 54$)	P
Median age of patients (range)	55 (26–68)	37 (18–53)	< 0.0001
Median age of donors (range)	50 (17–69)	34 (19–54)	< 0.0001
Male/female patient	57[1]/34	22/32	0.015
Female donor for male patient	19	10	0.83
Diagnosis AML (+ MDS)	27 (9)	17 (4)	0.0029
MDS	17	4	
CML	7	12	
ALL	1	8	
ML	36	13	
Others[2]	3	0	
Disease risk group (standard/advanced)[3]	14/77	21/33	0.0023
Median time interval[4] (range), (months)	19 (2–178)	10 (1–100)	0.014
KPS[5] ≤ 80%	10	5	0.41
HCT-SCI[6] ≥ 2	13	7	0.99
Prior infectious complications	6	3	0.99
Prior autologous transplantation	5	2	0.99
Donor type and source of stem cells			
Related PBSC/Unrelated BM	82/9	34/20	0.0002
GVHD prophylaxis			
CSP or TAC alone/MTX with CSP or TAC	66/25	1/53	< 0.0001
Acute GVHD grade II/III/IV	24/23/3	18/8/2	0.072
Median onset day (range) of grades II–IV acute GVHD[7]	39 (12–97)	32 (14–91)	0.48
Prior use of PSL for acute GVHD			
0.5–<1.0/1.0–<2.0/ ≥ 2.0 mg of PSL/kg	5/34/18	4/13/9	0.27
Relapse/progressive disease following cGVHD	16	10	0.99
Cause of death	30	20	0.27
Infection	15[8]	7[8]	
Chronic GVHD	9[8]	8[8]	
Lungs/gastrointestinal tract/MOF/Others[9]	3/1/3/2	3/3/2/0	
Others[10]	3	6	
Progression	8	2	
Median follow-up (range), (months)	39 (5–73)	45 (15–79)	0.20

[1]Number of patients, unless indicated otherwise.
[2]Others = myelofibrosis ($n = 1$), chronic lymphocytic leukemia ($n = 1$), and multiple myeloma ($n = 1$).
[3]Patients who were considered standard risk with a diagnosis of AML + MDS or AML, or ALL in first complete remission, CML in first chronic phase, or untreated refractory anemia in MDS. All other conditions were considered to indicate advanced risk.
[4]Time from diagnosis to transplantation.
[5]KPS was evaluated before the start of the conditioning regimen, and was graded according to Karnofsky performance status score.
[6]HCT-SCI was evaluated before the start of the conditioning regimen, and was graded according to hematopoietic cell transplantation-specific comorbidity index (ref. 8).
[7]Time from occurrence of grades II–IV acute GVHD to transplantation.
[8]Total number of patients differs because 8 patients (RIC, 5; CIC, 3) died of both infection and chronic GVHD.
[9]Others = renal ($n = 1$) and liver ($n = 1$).
[10]Others = RIC: cerebral infarction ($n = 1$), secondary hepatocellular carcinoma ($n = 1$), infection following secondary allogeneic cord blood stem cell transplantation; CIC: acute myocardial infarction ($n = 1$), cerebral infarction ($n = 1$), drug-induced interstitial pneumonia ($n = 1$), infection following chemotherapy ($n = 1$), and suicide ($n = 2$).
RIC, reduced-intensity regimen; CIC, conventional-intensity regimen; AML, acute myeloid leukemia; MDS, myelodysplastic syndrome; CML, chronic myeloid leukemia; ALL, acute lymphoblastic leukemia; ML, malignant lymphoma; PBSC, peripheral blood stem cell; BM, bone marrow; CSP, cyclosporine; TAC, tacrolimus; MTX, methotrexate; GVHD, graft-versus-host disease; PSL, prednisolone; cGVHD, chronic graft-versus-host disease; MOF, multiple organ failure.

Table 1

Clinical characteristics of cGVHD

	RIC	CIC	*P*
Median onset day (range)[1]	100 (79–479)	109 (93–348)	0.51
Limited/extensive	5/86	1/53	0.41
De novo/quiescent/progressive	27/38/26	24/9/21	0.16
KPS score 1/2/3	61/16/8	46/2/2	0.045
Skin score 1/2/3	27/33/8	17/12/3	0.15
Mouth score 1/2/3	40/29/3	23/9/1	0.87
Eyes score 1/2/3	30/14/7	15/9/1	0.38
Gastrointestinal tract score 1/2/3	28/4/12	19/1/7	0.84
Liver score 1/2/3	7/23/44	6/13/24	0.89
Lungs score 1/2/3	6/8/4	8/7/1	0.26
Joints and fascia score 1/2/3	13/2/0	8/5/1	0.13
Genital tract score 1/2/3	1/0/0	0/0/0	0.99
Eosinophilia $>0.5 \times 10^9$/L	30	22	0.37
Platelets $<100 \times 10^9$/L	26	20	0.36
Others[2]	5	2	0.39
Immunosuppressive drugs at diagnosis of cGVHD			
CSA/TAC	66/3	37/3	0.76
<0.5/0.5–<1.0/1.0–<2.0/ ≥ 2.0 mg of PSL/kg	17/9/11/2	9/2/3/1	0.57
Initial treatment for cGVHD			
Addition or increased dose of CSA/TAC	69/7	41/4	0.99
<0.5/0.5–<1.0/1.0–<2.0/ ≥ 2.0 mg of PSL/kg	18/14/15/4	10/7/6/2	0.74
Median follow-up from diagnosis of cGVHD (range) (months)	39 (5–73)	45 (15–79)	0.26

[1]Time from occurrence of cGVHD to transplantation.
[2]Others = pleural effusion ($n = 4$), pericardial effusion ($n = 3$), ascites ($n = 3$), and polymyositis ($n = 1$).
RIC, reduced-intensity regimen; CIC, conventional-intensity regimen; cGVHD, chronic graft-versus-host disease; KPS, Karnofsky performance status; CSP, cyclosporine; TAC, tacrolimus; PSL, prednisolone.

Table 2

infections consisted of exit site infections without bacteremia. Bacterial pneumonia was included in the category of definite infections, and was diagnosed by chest x-ray examination or computed tomography (CT) and identification of a bacterial pathogen on culture of sputum, bronchoalveolar lavage fluid, pleural fluid, or blood specimen. Fungal infections, including proven or probable invasive fungal infections, were diagnosed by identification of a fungal pathogen on culture or *Aspergillus* antigen and CT examination according to consensus criteria (13). Pneumonia of unknown origin was included in the category of undefined pneumoniae, which were diagnosed by chest x-ray and/or CT. There was no significant difference in CMV serostatus between the RIC and CIC groups (data not shown). A polymicrobial infection of 1 organ or several adjacent organs was considered to be a single infection. Death associated with a documented infection was defined as the death of a patient with findings consistent with an infection, or as detection of the pathogen in an autopsy specimen.

Statistical analysis

Comparisons of variables were performed using the 2-tailed Fisher exact test or the χ^2 test. Continuous variables were compared by the Mann–Whitney *U*-test. All *P*-values were 2-sided, and the type I error rate was fixed at $P < 0.05$.

Results

Transplant outcomes

The transplant outcomes are summarized in Table 1. Twenty-two patients (RIC, $n = 15$; CIC, $n = 7$) died of infections, of whom 8 patients (RIC, $n = 5$; CIC, $n = 3$) died of

both infections and chronic GVHD, with cGVHD at a median follow up of 40 months from transplantation (RIC, 39 vs. CIC, 45 months). The median onset of cGVHD was 112 days (RIC, 100 vs. CIC, 109 days), and 47 patients (RIC, $n = 26$; CIC, $n = 21$) developed progressive-type cGVHD at a median follow up of 32 months from diagnosis of cGVHD (RIC, 39 vs. CIC, 45 months). The severity of the Karnofsky performance status (KPS) score was significantly greater in the RIC group ($P = 0.045$).

Infectious complications

A total of 134 infectious episodes occurred in 83 patients (RIC, 51 vs. CIC, 32; $P = 0.73$), as shown in Table 3. Of these, 28 patients (RIC, 18 vs. CIC 10; $P = 0.83$) developed bacteremia, the causative organisms (43 positive cultures) of which are summarized in Table 4. Gram-positive bacteremia (27 positive cultures) was more common than gram-negative bacteremia (16 positive cultures). The bacteremia was caused by 2, 3, and 4 types of organisms in 4, 4, and 1 patient, respectively. The incidence of bacteremia was significantly higher in patients with the following factors: cGVHD including progressive types ($n = 15$, $P = 0.0027$), a KPS score ≥ 2 ($n = 11$, $P = 0.0062$) and a gastrointestinal (GI) score ≥ 2 ($n = 13$, $P < 0.0001$); PSL dose ≥ 1 mg/kg at the time of diagnosis ($n = 9$, $P = 0.00090$) and for the initial treatment of cGVHD ($n = 11$, $P = 0.0050$). CVC-related infections ($n = 11$) were caused by *Staphylococcus epidermidis* ($n = 4$), *Staphylococcus* species ($n = 2$), *Stenotrophomonas maltophilia* ($n = 2$), *Acinetobacter iwoffii* ($n = 1$), *Corynebacterium* species ($n = 1$), or methicillin-resistant *Staphylococcus aureus* (MRSA, $n = 1$). The incidence of CVC-related infections was significantly higher in patients with PSL dose ≥ 1 mg/kg at the time of diagnosis of cGVHD ($n = 4$, $P = 0.026$). Bacterial pneumonia was observed in 4 patients, and the isolated organisms were as follows: *Pseudomonas aeruginosa* ($n = 1$), *Hemophilus influenzae* ($n = 1$), *S. epidermidis* ($n = 1$), and *Staphylococcus* species ($n = 1$). The incidence of bacterial pneumonia ($n = 4$) was significantly higher in patients with PSL dose ≥ 1 mg/kg at the time of diagnosis ($n = 3$, $P = 0.0051$) and for the initial treatment of cGVHD ($n = 3$, $P = 0.021$). Invasive aspergillosis (IA) and *Candida* infections developed in 7 and 3 patients, respectively. All patients with IA had been given ≥ 0.5 mg of PSL/kg at the time of diagnosis of cGVHD. The incidence

Infectious complications associated with cGVHD

	Total (median onset, range, days)	RIC	CIC	*P*
Bacterial infections				
Bacteremia	28 (175, 104–1629)	18 (5)[1]	10 (2)	0.83
CVC-related	11 (123, 101–1774)	5 (0)	6 (0)	0.33
Pneumonia	4 (311, 101–1045)	3 (2)	1 (1)	0.99
Others[2]	16 (302, 102–1065)	7 (4)	9 (2)	0.11
Fungal infections				
Candida infection	3 (128, 101–358)	1 (0)	2 (0)	0.56
Invasive aspergillosis	7 (181, 112–1232)	6 (0)	1 (0)	0.26
Viral infections				
Adenoviral hemorrhagic cystitis	8 (192, 111–538)	5 (0)	3 (0)	0.99
CMV colitis	1 (343)	0 (0)	1 (0)	0.37
Cutaneous VZV	18 (502, 106–1684)	12 (0)	6 (0)	0.80
Influenza	4 (483, 355–898)	1 (0)	3 (0)	0.15
Others[3]	2 (133, 103–164)	1 (0)	1 (0)	0.99
CMV antigenemia	15 (140, 104–448)	11 (0)	4 (0)	0.42
Pneumoniae of unknown origin	32 (283, 101–1735)	18 (4)	14 (4)	0.41

[1]Number of infectious episodes (number of deaths) is shown.
[2]Others = sepsis of unknown origin (4 episodes), dermatitis (3), hemorrhagic cystitis (2), otitis media (2), meningitis (2), cholecystitis (1), pseudomembranous enterocolitis (1), and urinary tract infection (1).
[3]Others = herpes simplex viral esophagitis (1 episode) and meningitis (1).
cGVHD, chronic graft-versus-host disease; RIC, reduced-intensity regimen; CIC, conventional-intensity regimen; CVC, central venous catheter; CMV, cytomegalovirus; VZV, varicella zoster virus.

Table 3

Bacteremia associated with cGVHD

	RIC ($n = 18$)	CIC ($n = 10$)
Gram-positive organisms	16[1]	11
Staphylococcus epidermidis	7	2
Streptococcus species	2	3
Enterococcus species	3	0
Staphylococcus species	0	3
Bacillus species	0	1
Corynebacterium species	1	0
MRSA	0	1
Gram-positive cocci	3	1
Gram-negative organisms	10	6
Bacteroides species	3	2
Pseudomonas aeruginosa	2	2
Klebsiella species	2	0
Enterobacter species	0	1
Escherichia coli	0	1
Gram-negative rods	3	0

[1]Number of positive cultures.
cGVHD, chronic graft-versus-host disease; RIC, reduced-intensity regimen; CIC, conventional-intensity regimen; MRSA, methicillin-resistant *Staphylococcus aureus*.

Table 4

of IA was significantly higher in patients with cGVHD including a GI score ≥ 2 ($n = 4$, $P = 0.015$), PSL dose ≥ 1 mg/kg at the time of diagnosis ($n = 4$, $P = 0.0037$), and for the initial treatment of cGVHD ($n = 7$, $P < 0.0001$). Eighteen patients developed cutaneous varicella zoster virus (VZV); all responded promptly to acyclovir. Eight patients developed adenoviral hemorrhagic cystitis (HC); 2 of these 8 patients developed continuously complicated lethal bacteremia. The incidence of adenoviral HC was significantly higher in patients with cGVHD including a KPS score ≥ 2 ($n = 5$, $P = 0.0071$) and a GI score ≥ 2 ($n = 4$, $P = 0.026$); PSL dose ≥ 1 mg/kg at the time of diagnosis ($n = 4$, $P = 0.0069$); and for the initial treatment of cGVHD ($n = 5$, $P = 0.0060$). *De novo* CMV antigenemia before or after development of cGVHD was observed in 62 and 15 patients, respectively. Sixteen and 8 patients, respectively, died of bacterial infections and pneumoniae of unknown origin.

Discussion

In the present retrospective analysis, 57% (83/145) of patients with cGVHD developed infections, with a mortality rate of 27% (22/83). Although the limitations of this study were the retrospective study design and the differences in baseline characteristics in both the RIC and CIC groups, these results illustrate the importance of establishing more effective management of infectious complications associated with cGVHD, which are predictive of poor outcome for both RIC and CIC regimens.

In patients with cGVHD, the major source of bacteremia was heterogeneous, gram-positive organisms such as *S. epidermidis* and *Streptococcus* species, which were more common than gram-negative organisms, and bacteremia caused by *Pseudomonas aeruginosa*, including multidrug-resistant *P. aeruginosa*, occurred only in patients with cGVHD involving a GI tract score ≥ 2. Additionally, *Streptococcus pneumonia* sepsis was a risk factor for non-relapse mortality, as reported previously (4), and pneumococcal vaccination of transplant recipients was found to be relatively ineffective in the presence of cGVHD. In other studies with RIC regimens, the incidence of bacteremia appeared to be significantly lower than in the present study, but this may a result of the shorter follow-up periods in those studies (14, 15). Moreover, 29% (7/24) of the present patients with cGVHD involving a GI tract score ≥ 2 had received ≥ 2 mg of PSL/kg before developing cGVHD, and all 7 of these patients developed bacteremia. Although 50% (14/28) of patients with bacteremia received antibiotic

drugs and all 14 of these patients received intravenous immunoglobulin to maintain IgG levels at >400 mg/dL for prophylaxis of encapsulated bacteria and *Pneumocystis*, these results suggest that patients with cGVHD having a GI tract score ≥2, especially after high-dose PSL, are more likely to develop bacteremia than patients with cGVHD not having a GI tract score ≥2. This was probably due to colonization of the GI tract resulting from translocation into the bloodstream or disruption of the ecologic GI equilibrium involving GI bacterial overgrowth (e.g., use of antibiotic decontamination), increased permeability of the GI mucosal barrier (e.g., GVHD-induced mucosal damage), or deficiencies in the host immune defenses (e.g., use of immunosuppressive drugs). Thus, a review of strategies for prevention of bacteremia may lead to improvement of patient outcomes after allogeneic HSCT. That is, in patients with cGVHD having a GI tract score ≥2, restrictions on the use of broad-spectrum antibiotics may help reduce GI bacterial overgrowth, including overgrowth by antibiotic-resistant organisms, resulting from failure of the GI barrier. In contrast, we recognize the difficulty in identifying bacteremia using culturing blood. Our patients were immunocompromised hosts who presented with undifferentiated fever; therefore, blood culture results were often delayed well into the course of empirical therapy. There is a need to develop suitable strategies for screening of bacteremia associated with cGVHD in patients who receive allogeneic HSCT with either RIC or CIC regimens.

Most of the present patients with cGVHD who developed *Candida* infection or IA received ≥0.5 mg of PSL/kg before developing cGVHD and the incidence of IA was significantly higher in patients with cGVHD having a GI score ≥2, especially after high-dose PSL. The number of patients with fungal infections was small, but high-dose PSL may be effective for improving the prophylaxis for such infections. Furthermore, the duration of prophylaxis still remains unclear as randomized clinical trials have yet to be conducted.

All the present patients with adenoviral HC developed grades II–IV acute GVHD and received PSL for GVHD therapy, which differs considerably from what has been reported previously(16). The incidence of adenoviral HC was significantly higher in patients with cGVHD having a KPS score ≥2, a GI score ≥2, and high-dose PSL at the time of diagnosis and for the initial treatment of cGVHD. Although the present study was limited in its ability to detect risk factors for adenoviral HC, because of low patient numbers and lack of prospective investigation of viral infection, the present results suggest that patients who receive high-dose PSL before and after developing cGVHD should be frequently checked for abdominal and urinary symptoms, and that urinary tests should be regularly performed during ongoing use of immunosuppressive drugs. In addition, we identified only 1 patient with cGVHD who suffered from CMV colitis, indicating that it is useful to monitor and treat CMV antigenemia intensively in patients receiving immunosuppressive drugs, especially before development of cGVHD. In contrast, 12% of the present patients with cGVHD developed cutaneous VZV with a median onset of 502 days (range, 106–1684), despite low-dose acyclovir prophylaxis during at least the first year after allogeneic HSCT. Nonetheless, there were no cases of breakthrough VZV infection. This suggests that low-dose acyclovir prophylaxis effectively prevented breakthrough VZV infection, but that reestablishment of antiviral therapy was needed to protect against cutaneous VZV in patients with cGVHD.

In summary, the present data indicate that infections associated with cGVHD, especially after high-dose PSL, are predictive of poor outcome, whether RIC or CIC is used. Accordingly, there is a need for clinical trials to develop new strategies for screening and prevention of infections associated with cGVHD in patients who receive allogeneic HSCT with either RIC or CIC regimens.

References

1. Perez-Simon JA, Diez-Campelo M, Martino R, et al. Influence of the intensity of the conditioning regimen on the characteristics of acute and chronic graft-versus-host disease after allogeneic transplantation. Br J Haematol 2005; 130: 394–403.
2. Hori A, Kami M, Kim SW, et al. Development of early neutropenic fever, with or without bacterial infection, is still a significant complication after reduced-intensity stem cell transplantation. Biol Blood Marrow Transplant 2004; 10: 65–72.
3. Kojima R, Tateishi U, Kami M, et al. Chest computed tomography of late invasive aspergillosis after allogeneic hematopoietic stem cell transplantation. Biol Blood Marrow Transplant 2005; 11: 506–511.
4. Kulkarni S, Powles R, Treleaven J, et al. Chronic graft versus host disease is associated with long-term risk for pneumococcal infections in recipients of bone marrow transplants. Blood 2000; 95: 3683–3686.
5. Dykewicz CA. Summary of the guidelines for preventing opportunistic infections among hematopoietic stem cell transplant recipients. Clin Infect Dis 2001; 33: 139–144.
6. Sepkowitz KA. Opportunistic infections in patients with and patients without acquired immunodeficiency syndrome. Clin Infect Dis 2002; 34: 1098–1107.
7. Atsuta Y, Suzuki R, Yamamoto K, et al. Risk and prognostic factors for Japanese patients with chronic graft-versus-host disease after bone marrow transplantation. Bone Marrow Transplant 2006; 37: 289–296.
8. Sorror ML, Maris MB, Storb R, et al. Hematopoietic cell transplantation (HCT)-specific comorbidity index: a new tool for risk assessment before allogeneic HCT. Blood 2005; 106: 2912–2929.
9. Kanda Y, Mineishi S, Saito T, et al. Long-term low-dose acyclovir against varicella-zoster virus reactivation after allogeneic hematopoietic stem cell transplantation. Bone Marrow Transplant 2001; 28: 689–692.

10. Doney KC, Weiden PL, Storb R, Thomas ED. Treatment of graft-versus-host disease in human allogeneic marrow graft recipients: a randomized trial comparing antithymocyte globulin and corticosteroids. Am J Hematol 1981; 11: 1–9.
11. Shulman HM, Sullivan KM, Weiden PL, et al. Chronic graft-versus-host syndrome in man. A long-term clinicopathologic study of 20 Seattle patients. Am J Med 1980; 69: 204–217.
12. Filipovich AH, Weisdorf D, Pavletic S, et al. National Institutes of Health consensus development project on criteria for clinical trials in chronic graft-versus-host disease: I. Diagnosis and staging working group report. Biol Blood Marrow Transplant 2005; 11: 945–956.
13. Ascioglu S, Rex JH, De Pauw B, et al. Defining opportunistic invasive fungal infections in immunocompromised patients with cancer and haematopoietic stem cell transplants: an international consensus. Clin Infect Dis 2002; 34: 7–14.
14. Junghanss C, Marr KA, Carter RA, et al. Incidence and outcome of bacterial and fungal infections following nonmyeloablative compared with myeloablative allogeneic hematopoietic stem cell transplantation: a matched control study. Biol Blood Marrow Transplant 2002; 8: 512–520.
15. Busca A, Locatelli F, Barbui A, et al. Infectious complications following nonmyeloablative allogeneic hematopoietic stem cell transplantation. Transpl Infect Dis 2003; 5: 132–139.
16. El-Zimaity M, Saliba R, Chan K, et al. Hemorrhagic cystitis after allogeneic hematopoietic stem cell transplantation: donor type matters. Blood 2004; 103: 4674–4680.

Superior and Basal Segment Lung Cancers in the Lower Lobe Have Different Lymph Node Metastatic Pathways and Prognosis

Shun-ichi Watanabe, MD, Kenji Suzuki, MD, and Hisao Asamura, MD

Division of Thoracic Surgery, National Cancer Center Hospital, Tokyo, Japan

Background. Although the lower lobe is a large entity that occupies half of the hemithorax, all tumors located within the lower lobe have been treated uniformly regardless of tumor location. The aim of this study was to reveal differences in the metastatic pathway to the mediastinum and in prognosis of N2 disease between lung cancers originating from superior and basal segment of the lower lobe.

Methods. Data on 139 patients who underwent pulmonary resection with systematic nodal dissection for pN2 non-small cell lung cancer (NSCLC) originating from the lower lobe between 1980 and 2001 were retrospectively reviewed. Those lower lobe N2 tumors were divided into two groups by origin: 51 were superior segment, and 88 were basal segment.

Results. The superior segment group showed a significantly higher incidence of superior mediastinal metastasis than the basal segment group (64% vs 36%, $p = 0.0012$). When superior mediastinal metastasis existed, the basal segment group showed a significantly higher incidence of synchronous subcarinal metastasis than the superior segment group (81% vs 39%, $p = 0.0006$). Pneumonectomy was required significantly more often in the superior segment group than in the basal segment group (45% vs 17%, $p = 0.0003$). The basal segment origin tumors with only subcarinal metastasis showed significantly better prognosis than other lower lobe N2 tumors (5-year survival, 43% vs 18%; $p = 0.0155$).

Conclusions. Basal segment tumor metastasizes to the superior mediastinum mostly through the subcarinal node, whereas superior segment tumors often metastasize directly to the superior mediastinum without concomitant metastasis to the subcarinal node. Superior mediastinal dissection will be mandatory for accurate staging of superior segment tumors even when the subcarinal node is negative on frozen section. As for the prognosis among lower lobe N2 tumors, only in cases with basal segment tumor without superior mediastinal metastasis may long-term survival be expected.

(Ann Thorac Surg 2008;85:1026–31)

The lower lobe is a large entity that occupies half of the hemithorax in each side. Its bottom rests just on the diaphragm and the apex reaches above the hilum. However, all tumors located within the lower lobe have been treated uniformly, regardless of location in the lobe. With respect to the anatomic structure, the lower lobe can be primarily divided into two segments, the superior and the basal. We hypothesized that tumors arising in those two lower lobe segments were not alike owing to differences in lymphatic drainage pathways or other clinical behaviors and thus may require different treatment strategies. We therefore investigated segment-specific patterns of nodal spread and prognosis of pN2 disease in each segment. This report describes the differences in the clinical features and prognosis between superior and basal segment tumor of the lower lobe.

Accepted for publication Oct 23, 2007.

Address correspondence to Dr Watanabe, Division of Thoracic Surgery, National Cancer Center Hospital, Tsukiji 5-1-1, Tokyo 104 0045, Japan; e-mail: syuwatan@ncc.go.jp.

0003-4975/08/$34.00
doi:10.1016/j.athoracsur.2007.10.076

Patients and Methods

Patients

Approval for this retrospective study was obtained and the need for individual patient consent was waived by the Institutional Review Board. From January 1981 to December 2001, 3638 patients underwent pulmonary resection for primary lung cancer at the National Cancer Center Hospital. Basically, we operate on the lung cancer patient who is considered to be cN0 to 1 on computed tomography (CT) scan. Our criterion for lymph node enlargement is more than 1.0 cm in the short axis of each nodal station on CT. Mediastinoscopy, mediastinotomy, or positron emission tomography scan were not routinely used preoperatively.

We retrospectively reviewed 139 patients (3.8%) who underwent at least lobectomy and systematic nodal dissection (SND) for lower lobe tumor in either the right or left lung and who had histologic evidence of non-small cell lung cancer (NSCLC) with mediastinal lymph node metastasis (pN2). We excluded the patients who underwent only sampling or selective nodal dissection. The study excluded tumors that crossed the fissure and invaded multiple lobes or other organs and huge tumors

Table 1. Patient Characteristics in Pathologic N2 Non-Small Cell Lung Cancer Originating From the Lower Lobe

Patients, No.	139
Age, mean ± SD year (range)	60 ± 11 (26–85)
Sex, No (%)	
Male	95 (68)
Female	44 (32)
Histological type, No (%)	
Adenocarcinoma	94 (68)
Squamous cell carcinoma	37 (27)
Others	8 (5)
Primary tumor location, No (%)	
Superior segment	51 (37)
Right	35
Left	16
Basal segment	88 (63)
Right	51
Left	37

more than 5 cm in size. All patients underwent at least lobectomy with hilar and mediastinal lymphadenectomy.

Patients were subdivided into two groups according to origin: superior segment (n = 51) and basal segment (n = 88). The correlation between the segment of the tumor location and the involved hilar/mediastinal nodes were investigated in each case. The location of the tumor was identified by the involved bronchus in the resected specimen. When the tumor involved both the superior and the basal segments, the patient was placed in the superior segment group.

Surgical Procedure

Pulmonary resection and systematic nodal dissection were performed through posterolateral thoracotomy. At thoracotomy, the diagnosis was confirmed by frozen-section analysis when histologic confirmation was not available preoperatively. When the hilar nodes involved the upper lobe bronchus or pulmonary artery, or both, pneumonectomy was done. Systematic nodal dissection, including the superior and inferior mediastinum, was then performed after pulmonary resection. In left thoracotomy, superior mediastinal lymph nodes indicated the 5, 6, and 4L nodes. In right thoracotomy, superior mediastinal lymph nodes indicated the 1, 2R, and 4R nodes. Inferior mediastinal lymph nodes indicated the 7, 8, and 9 nodes in both side thoracotomies. Histologic analysis of lymph node metastasis was made by hematoxylin and eosin stain.

Statistical Analysis

Survival was calculated by the Kaplan-Meier method, and differences in survival were determined by the log-rank test. Zero time was the date of surgery, and the terminal events were death due to cancer, noncancer, or unknown causes. A multivariable analysis of independent prognostic factors was done by using Cox's proportional hazards regression model. Relative risk and 95% confidence intervals were calculated. Proportions were compared by means of χ^2 analysis. Values of $p < 0.05$ were considered to be statistically significant.

Results

Patient Characteristics

Patient characteristics are summarized in Table 1. The tumor cell types were adenocarcinoma in 94 (68%), squamous cell carcinoma in 37 (27%), and others in 8 (5%). The segments of origin were the superior segment in 51 (37%), in 35 of whom the tumor was on the right side, and basal segment in 88 (63%), in 51 of whom the tumor was on the right side. The size of the primary tumor was less than 3 cm in 65 patients (47%).

Patterns of Nodal Spread

Significant differences in patterns of lymphatic pathways on both sides were found when the superior and basal segment groups were compared (Table 2). The basal segment group showed significantly higher incidence of subcarinal metastasis than the superior segment group (80% vs 57%, $p = 0.0044$). The superior segment group showed significantly higher incidence of superior mediastinal metastasis than the basal segment group (64% vs 36%, $p = 0.0012$; Table 2). When superior mediastinal metastasis existed, the basal segment group showed a significantly higher incidence of synchronous subcarinal metastasis than did the superior segment group (81% vs 39%, $p = 0.0006$; Table 3).

Table 2. Location of the Primary Tumor in the Lower Lobe and Incidence of Subcarinal and Superior Mediastinal Node Involvement

			Metastasis to the Subcarinal Node		Metastasis to the Superior Mediastinal Node	
Side	Primary Tumor Location	Patients, No.	No. (%)	*p* Value	No. (%)	*p* Value
Right	Superior segment	35	22 (63)	0.0229	22 (63)	0.0118
	Basal segment	51	43 (84)		18 (35)	
Left	Superior segment	16	7 (44)	0.0417	11 (69)	0.0385
	Basal segment	37	27 (73)		14 (38)	
Total	Superior segment	51	29 (57)	0.0044	33 (64)	0.0012
	Basal segment	88	70 (80)		32 (36)	

Ann Thorac Surg
2008;85:1026–31

Table 3. Location of the Primary Tumor in the Lower Lobe and Incidence of Synchronous Metastasis to the Superior Mediastinal and Subcarinal Nodes

Side	Primary Tumor Location	Patients With Superior Mediastinal Involvement, No.	Synchronous Metastasis to the Subcarinal Node	
			No. (%)	*p* Value
Right	Superior segment	22	9 (41)	0.0064
	Basal segment	18	15 (83)	
Left	Superior segment	11	4 (36)	0.0325
	Basal segment	14	11 (79)	
Total	Superior segment	33	13 (39)	0.0006
	Basal segment	32	26 (81)	

Differences in Surgical Procedure

The superior segment group more frequently required pneumonectomy than the basal segment group, with a significant difference (45.1% vs 17.0%, $p = 0.0003$), but there was no significant difference in the ratio of T1/T2 between the groups (24 of 21 vs 41 of 47, $p = 0.9021$; Table 4).

Group Differences in Prognosis of N2 Disease

Overall 5-year survival of patients with lower lobe N2 tumor was 27.9%. The 5-year survival of the basal segment group was better than for the superior segment group (32.9% vs 19.9%); however, the difference was not significant ($p = 0.1308$; Fig 1).

Among the basal segment group, the patients without superior mediastinal metastasis showed significantly better prognosis than did those with it, with a 5-year survival of 42.7% vs 15.6% ($p = 0.0453$; Fig 2A).

In the superior segment group, no significant differences in survival were detected between patients with and without superior mediastinal metastasis: at 5 years, the survival was 25.4% for those without and 16.5% for those with, survival with only superior mediastinal node metastasis was 20.0%; and with superior mediastinal and subcarinal metastasis, 10.3% ($p = 0.1623$; Fig 2B).

Collectively, the basal segment origin tumors with only subcarinal metastasis showed significantly better prognosis than other lower lobe N2 tumors (5-year survival 43% vs 18%, $p = 0.0155$).

Comment

The lower lobe has a large volume of lung parenchyma, including 5 segments in the right and 4 segments in the left, and occupies half of the hemithorax in each side. Despite the extensive size of the lower lobe, all tumors located there have been treated similarly, regardless of whether the tumor originated in the superior or the basal segments. Owing to a lack of information on the variations in clinicopathologic features between tumors located in the superior and basal segments, we conducted the present study to investigate the differences in patterns of lymph node metastasis and prognosis of each segment.

Our results on the metastatic pathway showed a possibility that basal segment tumors metastasizing to the superior mediastinum mostly went through the subcarinal node, whereas SS tumors often metastasized directly to the superior mediastinum without concomitant metastasis to the

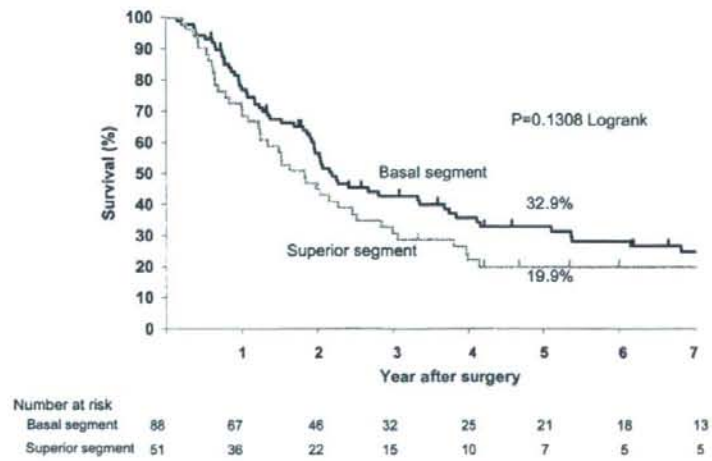

Fig 1. Survival of patients with pN2 tumors located in the basal and superior segment of the lower lobe. The 5-year survival was 32.9% for the basal segment group (black line) and 19.9% for the superior segment group (gray line), but the difference was not significant ($p = 0.1308$).

Table 4. Types of Surgical Procedure for Lower Lobe pN2 Disease According to the Segment of the Primary Tumor in the Lower Lobe

Primary Tumor Location of the	Patients, No.	Surgical Procedure, No. (%)		T Status (T1/T2)
		Pneumonectomy	Lobectomy	
Superior segment	51	23 (45.1)[a]	28 (54.9)	24/27[b]
Basal segment	88	15 (17.0)[a]	73 (83.0)	41/47[b]
Total	139	38 (27.3)	101 (72.7)	65/74

[a] $p = 0.0003$; [b] $p = 0.9021$.

subcarinal node (Tables 2 and 3). Furthermore, the patterns of metastatic pathway in the right and left side were identical (Tables 2 and 3). The schemes demonstrating a possibility of the main stream of lymphatic spread in each segment on the basis of these results are shown in Figure 3. Perhaps superior segment tumors tend to metastasize directly to the upper mediastinum owing to the anatomically shorter distance between these sites compared with the longer distance between the basal segment and the upper mediastinum. Alternatively, for basal segment tumors, the subcarinal node could be a barrier on its metastatic way to the upper mediastinum.

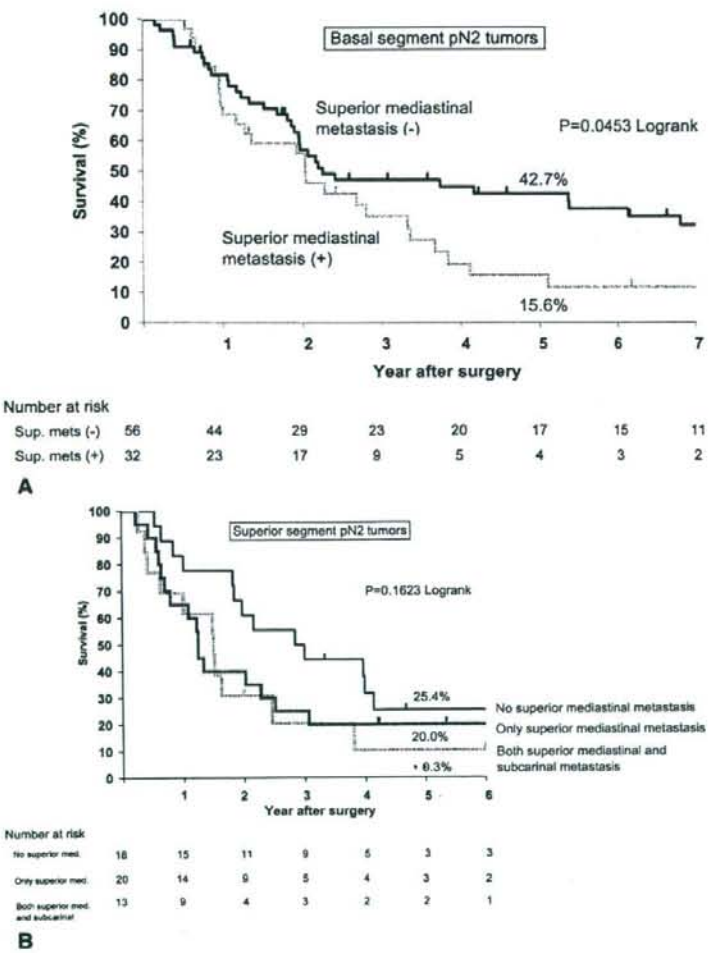

Fig 2. Survival of patients with lower lobe pN2 tumors with and without superior mediastinal metastasis in tumors with (A) basal segment origin and (B) superior segment origin. (A) In the basal segment group, the patients without superior mediastinal metastasis (black line) showed significantly better prognosis than did those with (grey line) superior mediastinal metastasis (5-year survival, 42.7% vs 15.6%, $p = 0.0453$). (B) Survival of patients with superior segment pN2 tumors grouped by the extent of lymph node metastasis. No significant differences in survival were detected between patients without superior mediastinal metastasis (black line; 5-year survival, 25.4%) and with superior mediastinal metastasis (5-year survival, 16.5%: with only superior mediastinal node metastasis (dark gray line, 20.0%; with superior mediastinal and subcarinal metastasis, light gray line, 10.3%; $p = 0.1623$).

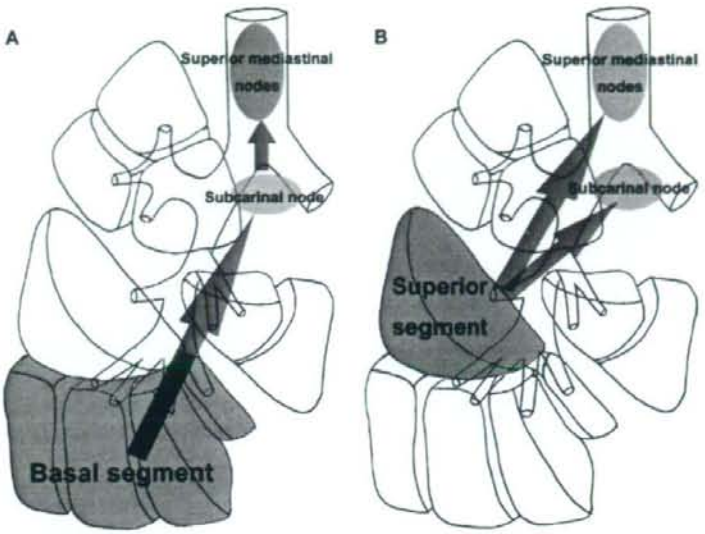

Fig 3. The scheme of the main stream of lymphatic spread of the tumor in each segment. (A) Basal segment tumor metastasizes to the superior mediastinum mostly through the subcarinal node. (B) Superior segment tumor often metastasizes directly to the superior mediastinum, without concomitant metastasis to the subcarinal node.

These factors might contribute to the higher incidence of pneumonectomy in superior segment tumors than that in basal segment tumors. Probably in many patients in the superior segment group, interlobar nodes that were located on the way from the primary site to superior mediastinum were involved. That is, superior segment tumor seems to metastasize to the superior mediastinum by involving the nodes adjacent to the bronchus and pulmonary artery of the upper lobe in consideration of the anatomy of the hilum. Then, this point will lead to the high incidence of pneumonectomy in the superior segment group.

Extensive nodal dissection, including the superior and inferior mediastinum, has been universally performed in lung cancer operations [1, 2]. This technique, termed "systematic nodal dissection" remains an important component of the investigative and therapeutic process in all patients undergoing thoracotomy for lung cancer [3–5]. However, because the number of lung cancers detected early is increasing with the development of CTs scanners, a new therapeutic strategy for selective nodal dissection is required instead of systematic nodal dissection [6, 7]. The extent of nodal dissection could be tailored according to the tumor location–specific patterns of nodal spread [8].

Riquet and associates [9] reported that lung cancer metastasizes so easily to the mediastinum that selection of the patients for limited surgical intervention should be discussed carefully. Some previous reports have described the appropriateness of selective nodal dissection based on the lobe-specific extent of nodal spread [7, 10, 11]. Okada and associates [11] reported that superior mediastinal dissection might be unnecessary for lower lobe tumors when the subcarinal node was negative. Our results support their conclusion for basal segment tumor; however, for the superior segment tumor, our results reveal that superior mediastinal dissection should be mandatory for accurate staging even when the subcarinal node is negative.

The prognosis for patients with superior segment tumors was worse, with a 5-year survival of 20% compared with 33% for patients with basal segment tumors, although this difference was not statistically significant. Poor survival rates may be attributed to the increased incidence of pneumonectomy in superior segment tumors (45%) compared with 17% for basal segment tumors (Table 4). Although the prognoses of patients with superior mediastinal metastasis from superior and basal segment tumors of the lower lobe were dismal, with respective 5-year survivals of 17% and 16%, the patients with basal segment N2 tumors who had only subcarinal metastasis showed significantly better 5-year survival of 43%, an acceptable result, compared with other lower lobe N2 patients. This will be mainly because they have metastasis to a single N2 station with an anatomically shorter distance from the primary site. Only in this small subgroup of lower lobe N2 patients, those with tumors of basal segment origin and having no superior mediastinal metastasis, may long-term survival be expected.

References

1. Cahan WG. Radical lobectomy. J Thorac Cardiovasc Surg 1960;39:555–72.
2. Naruke T, Suemasu K, Ishikawa S. Lymph node mapping and curability at various levels of metastasis in resected lung cancer. J Thoracic Cardiovasc Surg 1978;76:832–9.
3. Graham AN, Chan KJ, Pastorino U, Goldstraw P. Systematic nodal dissection in the intrathoracic staging of patients with non-small cell lung cancer. J Thoracic Cardiovasc Surg 1999;117:246–51.
4. Keller SM, Adak S, Wagner H, Johnson DH. Mediastinal lymph node dissection improves survival in patients with

stage II and IIIa non-small cell lung cancer. Ann Thorac Surg 2000;70:358–66.
5. Oda M, Watanabe Y, Shimizu J, et al. Extent of mediastinal node metastasis in clinical stage I non-small-cell lung cancer: The role of systematic nodal dissection. Lung Cancer 1998;22:23–30.
6. Watanabe S, Oda M, Go T, et al. Should mediastinal nodal dissection be routinely undertaken in patients with peripheral small-sized lung cancer? Retrospective analysis of 225 patients. Eur J Cardiothorac Surg 2001;20:1007–11.
7. Naruke T, Tsuchiya R, Kondo H, Nakayama H, Asamura H. Lymph node sampling in lung cancer. How should it be done? Eur J Cardiothorac Surg 1999;16(suppl 1):17–24.
8. Watanabe S, Asamura H, Suzuki K, Tsuchiya R. The new strategy of selective nodal dissection for lung cancer based on segment-specific patterns of nodal spread. Interactive Cardiovascular and Thoracic Surgery 2005;4:106–9.
9. Riquet M, Hidden G, Debesse B. Direct lymphatic drainage of lung drainage of lung segments to the mediastinal nodes. J Thorac Cardiovasc Surg 1989;97:623–32.
10. Asamura H, Nakayama H, Kondo H, Tsuchiya R, Naruke T. Lobe-specific extent of systematic lymph node dissection for non-small cell lung carcinomas according to a retrospective study of metastasis and prognosis. J Thorac Cardiovasc Surg 1999;117:1102–11.
11. Okada M, Tsubota N, Yoshimura M, Miyamoto Y. Proposal for reasonable mediastinal lymphadenectomy in bronchogenic carcinomas: role of subcarinal nodes in selective dissection. J Thorac Cardiovasc Surg 1998;116:949–53.

The Society of Thoracic Surgeons Policy Action Center

The Society of Thoracic Surgeons (STS) is pleased to announce a new member benefit—the STS Policy Action Center, a website that allows STS members to participate in change in Washington, DC. This easy, interactive, hassle-free site allows members to:

- Personally contact legislators with one's input on key issues relevant to cardiothoracic surgery
- Write and send an editorial opinion to one's local media
- E-mail senators and representatives about upcoming medical liability reform legislation
- Track congressional campaigns in one's district—and become involved
- Research the proposed policies that help—or hurt—one's practice
- Take action on behalf of cardiothoracic surgery

This website is now available at www.sts.org/takeaction.

Lung Cancer (2008) 60, 125–131

available at www.sciencedirect.com

ScienceDirect

journal homepage: www.elsevier.com/locate/lungcan

SHORT COMMUNICATION

Mucoepidermoid carcinoma of the lung: High-resolution CT and histopathologic findings in five cases

Taichiro Ishizumi[a,b,*], **Ukihide Tateishi**[a], **Shun-ichi Watanabe**[b], **Yoshihiro Matsuno**[c]

[a] *Divisions of Diagnostic Radiology and Nuclear Medicine, National Cancer Center Hospital, 5-1-1, Tsukiji, Chuo-Ku, 104-0045 Tokyo, Japan*
[b] *Divisions of Thoracic Surgery, National Cancer Center Hospital, 5-1-1, Tsukiji, Chuo-Ku, 104-0045 Tokyo, Japan*
[c] *Divisions of Pathology, National Cancer Center Hospital, 5-1-1, Tsukiji, Chuo-Ku, 104-0045 Tokyo, Japan*

Received 13 December 2006; received in revised form 30 June 2007; accepted 21 August 2007

KEYWORDS
Mucoepidermoid carcinoma;
Lung;
High-resolution CT

Summary
Objective: The purpose of this study was to characterize the high-resolution computed tomography (HRCT) findings of mucoepidermoid carcinoma of the lung and correlate them with the histopathological features.
Methods: The study included five patients with pathologically proven mucoepidermoid carcinoma who underwent HRCT before treatment. The HRCT findings were then compared with the histopathological features in all patients.
Results: The HRCT images showed lesions in the central lung in four patients and in the peripheral lung in one. All the lesions were well defined nodules or masses with a smooth margin. The contour of the tumours was oval ($n = 3$), round ($n = 1$) or lobulated ($n = 1$). The contrast-enhanced CT images showed marked heterogeneous enhancement with foci of relatively low attenuation in four of the five lesions and mild heterogeneous enhancement in the other lesion. There was an admixed distribution of areas that are heterogeneous in the densities of blood vessels, as highlighted by immunohistochemical staining of CD31. Most mucin-secreting areas of the tumours showed more densely distributed blood vessels, mostly capillaries, in between tumour cell nests, whereas other areas did less. All five patients in our series underwent lobectomy plus lymph node dissection or sampling. All the patients are alive without evidence of disease an average of 50.4 months after surgery (range, 15–82 months; median, 57 months).

* Corresponding author at: Divisions of Diagnostic Radiology and Nuclear Medicine, National Cancer Center Hospital, 5-1-1, Tsukiji, Chuo-Ku, 104-0045 Tokyo, Japan. Tel.: +81 3 3542 2511; fax: +81 3 3542 3815.
E-mail address: tishizumi@hotmail.co.jp (T. Ishizumi).

0169-5002/$ – see front matter
doi:10.1016/j.lungcan.2007.08.022

Conclusion: Mucoepidermoid carcinoma of the bronchus is often visualized as marked heterogeneous contrast enhancement on HRCT images. The results of this study suggest that the presence of abundant microvessels, detected immunohistochemically by microscopic examination, affects the enhancement pattern on HRCT.

1. Introduction

Mucoepidermoid carcinoma of the lung is an extremely rare tumour, comprising less than 5% of primary bronchial tumours and 0.1–0.2% of all lung cancers [1–4]. The largest series (56 cases over 26 years) has been published by Yousem and Hochholzer [3]. These tumours are thought to originate from bronchial gland of minor salivary gland-type lining the bronchi, and are classified into low grade and high grade on the basis of histological criteria [1,3,5]. The most important factors in the prognosis include the histological grade and whether complete surgical resection is possible. Completely resectable low-grade tumours generally have an excellent prognosis [3,6].

The radiological appearance of mucoepidermoid carcinoma of the lung depends on tumour location, size and whether obstructive pneumonia is present. The reported computed tomographic (CT) appearance of mucoepidermoid carcinoma of the lung is a well circumscribed oval or lobulated mass arising within the bronchus [7]. Although some investigators have reported the CT features of this tumour [7–10], few reports have included detailed findings of high-resolution CT (HRCT) or correlated them with histopathologic features. The purpose of this study was to characterize the HRCT findings of mucoepidermoid carcinoma of the lung and correlate them with the histopathologic features.

2. Materials and methods

The patients investigated in this study presented at the National Cancer Center, Tokyo, Japan, for diagnosis and treatment during the period from January 1999 through December 2005. Only patients with primary mucoepidermoid carcinoma of the lung were included; patients with pulmonary metastasis from remote sites were excluded. Five patients underwent HRCT and were treated for primary mucoepidermoid carcinoma. The diagnosis was confirmed by histopathologic examination of the surgical specimen in all five patients. All clinical records, including the follow-up information, HRCT findings, endoscopic images and gross and microscopic specimens, were reviewed retrospectively.

2.1. HRCT protocols

HRCT was performed with either a 4-row or 16-row multi-detector CT (MDCT) scanner (Aquilion V-detector, Toshiba Medical Systems Corp., Tokyo Japan). The patients were evaluated with the MDCT scanner by using axial 2.0 mm × 4 mm or 16 modes, 120 kVp, 200–250 mA, and thin-section CT images were obtained using 1.0 mm sections reconstructed at 2.0 mm intervals with a high-spatial-frequency algorithm and retrospectively retargeted to each lung with a 20 cm field of view (FOV). All patients were intravenously injected with 80–150 ml of non-ionic contrast medium at a rate of 2.0–3.0 ml/s with an autoinjector (Autoenhance A-250, Nemoto Kyorindo, Tokyo, Japan), and scanning was started after a 40 s delay. Hard-copy images were photographed at window settings for the lung (center, −600 HU; width, 2000 HU) and the mediastinum (center, 35 HU; width, 400 HU). The intervals between the CT examinations and surgery ranged from 2 days to 4 weeks. All patients were followed up regularly in our institute. Follow-up CT images were obtained in all patients.

The HRCT images were assessed by two independent observers without reference to the clinical findings. The location of the pulmonary nodule was classified as peripheral or central. Nodules present within the peripheral two-thirds of the lung were arbitrarily classified as peripheral type and those within the central one-third or in contact with lobar or segmental bronchi were classified as central. The CT analysis included determination of the attenuation coefficient of the pulmonary lesion. CT attenuation coefficient was evaluated before and after administration of contrast media. The contrast enhancement of the tumour was compared with that of the chest wall musculature. Whether intratumoral calcification was present was also noted. After making independent initial evaluations, the two observers reviewed all cases in which their interpretations differed and reached a final consensus.

2.2. Histopathologic examination

Surgical specimens were inflated and fixed by transpleural and transbronchial infusion with formalin. The specimens were sectioned transversely in the same planes as the HRCT images, stained with hematoxylin-eosin and immunostained for the endothelial marker CD31. One of the authors, an experienced pulmonary pathologist, reviewed the histopathologic findings. The characteristics of the tumours on the HRCT images were compared with the histopathologic findings.

3. Results

3.1. Clinical features

The clinical data are summarized in Table 1. The five patients (two males and three females) ranged in age from 22 to 58 years, and their average age was 41.6 years. Only two of them were smokers. Four of the patients complained of chronic symptoms, including cough, increased sputum production and episodic fevers. These symptoms were related to bronchial irritation, partial or complete bronchial obstruction and distal pneumonia. The remain-

Table 1 Clinical data of patients with mucoepidermoid carcinoma of the bronchus

Case	Age (year)	Sex	Symptom	Tumour location	Tumour site	Preoperative diagnosis
1	22	M	Cough, sputum	Central	Lt. LLB (B6)	Mucoepidermoid Ca.
2	40	W	Fever, chest pain	Central	Rt. MLB	Mucoepidermoid Ca.
3	58	W	Cough, sputum, fever	Central	Rt. BB (B9)	Non-typed malignant tumour
4	51	M	None	Peripheral	Rt. MLB (B4a)	No malignancy
5	37	W	Cough, sputum, fever	Central	Lt. UDB	No biopsy

Lt. LLB, Left lower lobe bronchus; Rt. BB, right basal bronchus; Rt. MLB, right middle lobe bronchus; Lt. UDB, left upper division bronchus.

ing patient was asymptomatic, and the lesion was detected during routine health examination.

The serum sialyl Lewis X-i antigen (SLX) values were high in all five cases. The serum carcinoembryonic antigen (CEA) and carbohydrate antigen 19-9 (CA19-9) values were high in three cases. The serum cytokeratin fragment 19 (CYFRA 21-1), squamous cell carcinoma antigen (SCC), neuron specific enolase (NSE), progastrin-releasing peptide (pro-GRP) values were all within the normal range.

3.2. HRCT findings

On the CT images, the tumours ranged in diameter from 18 to 38 mm (mean, 28.4 mm) (Table 2). The lesions were located in the central lung in four cases and in the peripheral lung in one. All the lesions were well defined nodules or masses with a smooth margin (Fig. 1). The contour of the tumours was round ($n = 1$), oval ($n = 3$) or lobulated ($n = 1$). Non-enhanced CT scans revealed intratumoral punctate calcification in one of the five lesions (Case 1). CT findings suggestive of bronchial stenosis or obstruction were seen in all cases (distal obstructive pneumonia in four cases, distal bronchial dilation in four and atelectasis in three). Atelectasis with recurrent or non-resolving pneumonia was observed distal to the site of obstruction.

CT attenuation coefficients were evaluated before and after administration of contrast medium. Thus, the change of CT attenuation or the degree of contrast enhancement was described. CT images enhanced by intravenous contrast medium showed marked heterogeneous enhancement with foci of relatively low attenuation in four of the five lesions and mild heterogeneous enhancement in the other lesion. Measurement of Hounsfield unit (HU) data was possible in every patient. The attenuation coefficients of the four markedly enhanced tumours (range, 95–139 HU; mean, 118.5 HU) were much higher than those of the chest wall musculature (range, 48–68; mean, 61.3 HU), whereas that of the one mildly enhanced tumour was slightly higher than that of the chest wall musculature. The ratio of the attenuation coefficient of the tumour to that of the musculature in the mildly enhanced case was 1.5, whereas those of the markedly enhanced cases were much higher (range, 2.0–2.2) (Table 2). None of the patients had lymphadenopathy in the mediastinum, pulmonary hilum or around the bronchi, on the basis of the CT findings.

3.3. Bronchoscopic findings

Bronchoscopy was performed in all five cases and the tumours were easily visualized except the peripheral lesion. The tumours were located in the lobar or segmental bronchi and had filled the bronchial lumen. They were soft, polypoid with a sessile base and pink like the bronchial mucosa. Three of the tumours were covered by a highly vascular mucosa. Although bronchoscopic brushing or biopsy was performed in four cases, a preoperative diagnosis of mucoepidermoid carcinoma was made in only two of them. Bronchoscopy in the other two cases revealed a non-typed malignant tumour or non-diagnostic inflammatory cells.

3.4. Treatment

The treatment chosen for all patients was surgical resection, and the procedure consisted of routine lobectomy including right middle and lower lobectomy (Table 2). The surgical procedures resulted in tumour-free margins. Lymph node dissection or sampling of pulmonary hilar and mediastinal lymph nodes was performed in all cases.

3.5. Histopathologic findings

The histologic diagnosis was low-grade mucoepidermoid carcinoma in all five cases (Table 3). The central tumours

Table 2 HRCT findings of mucoepidermoid carcinoma of the bronchus in four patients

Case	Tumour size (mm)	Tumour margin	Tumour contour	Pattern of enhancement	Ratio of attenuation coefficient
1	38 × 35	Well defined (smooth)	Oval	Heterogeneous	2.1
2	26 × 18	Well defined (smooth)	Lobulated	Heterogeneous	1.5
3	34 × 22	Well defined (smooth)	Oval	Heterogeneous	2.1
4	24 × 24	Well defined (smooth)	Round	Heterogeneous	2
5	33 × 29	Well defined (smooth)	Oval	Heterogeneous	2.2

Ratio of attenuation coefficient: Ratio of the attenuation coefficient of the tumour to attenuation coefficient of the musculature

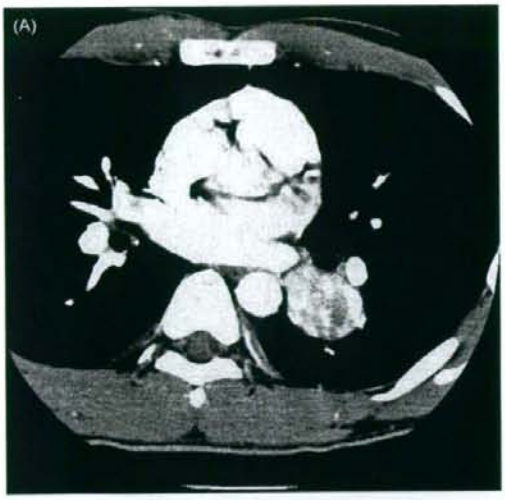

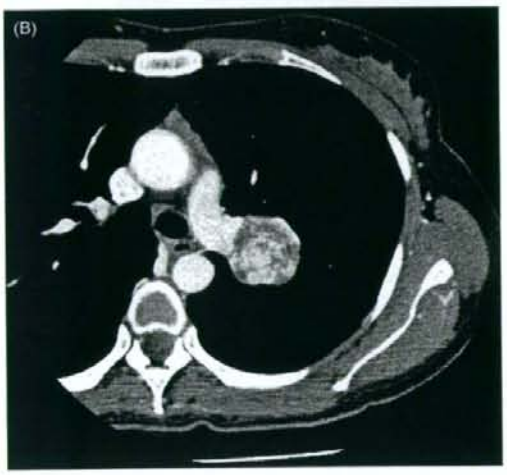

Fig. 1 Mucoepidermoid carcinomas of the bronchus were well defined mass and had a smooth margin. Enhanced CT images shows marked heterogeneous enhancement with foci of relatively low attenuation (A, Case 1; B, Case 5).

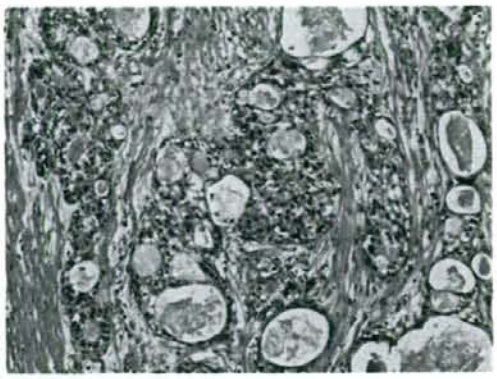

Fig. 2 High-magnification photomicrograph showed the epithelial component of the tumours consisted of mucin-secreting cells, squamoid cells and intermediate-type cells that displayed no specific differentiation.

protruded into the lumen of the bronchus and almost totally occluded it. On cut sections, the tumours were light yellow or tan polypoid masses. The margins and contours of the tumours were smooth, and they were well circumscribed and oval or round, consistent with their CT appearance.

Microscopically, the tumours were seen to arise from bronchial glands and to have infiltrated the bronchial wall. The epithelial component of the tumours consisted of mucin-secreting cells, squamoid cells and intermediate-type cells that displayed no specific differentiation (Fig. 2). Cystic change predominated in some areas, and the solid areas comprised mucin-secreting columnar epithelium that had formed small glands, tubules and cysts. There were no prominent nucleoli, and mitotic figures and necrosis were absent or minimal (less than five mitoses per 50 high-power fields). Keratinization was rare or absent in the epidermoid areas. These pathologic findings are characteristic of low-grade mucoepidermoid carcinoma. There was an admixed distribution of areas that are heterogeneous in the densities of blood vessels, as highlighted by immunohistochemical staining of CD31. Most mucin-secreting areas of the tumours showed more densely distributed blood vessels, mostly capillaries, in between tumour cell nests, whereas other areas did less (Fig. 3). Stromal calcification and ossification with a granulomatous reaction was observed in Case 1. The histologic specimens in Case 1, in which intratumoral punctate calcifications were observed on non-enhanced HRCT scans, showed microscopic calcification. Distal obstructive pneu-

Table 3 Histopathologic findings and outcome

Case	Treatment	p-Stage (TNM)	Grade	CD31	Outcome
1	Left lower lobectomy	T2N0M0 IB	Low-grade	(++)	NED
2	Right middle and lower lobectomy	T1N0M0 IA	Low-grade	(++)	NED
3	Right lower lobectomy	T2N0M0 IB	Low-grade	(+)	NED
4	Right middle lobectomy	T1N0M0 IA	Low-grade	(++)	NED
5	Light upper lobectomy	T2N0M0 IB	Low-grade	(++)	NED

NED: No evidence of disease.

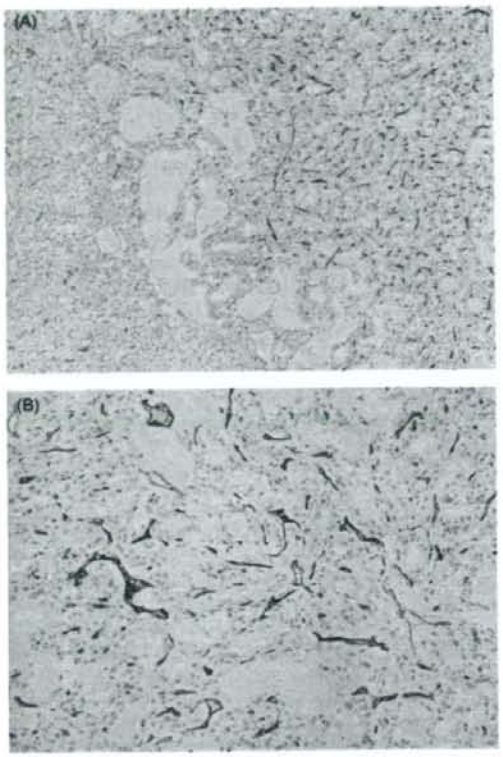

Fig. 3 (A) Immunohistochemical findings showing a border of areas with and without dense blood vessels as highlighted by anti-CD31 antibody. Note the abundant glands with mucus production in the right half, where there are more vessels labeled by anti-CD31 antibody. (B) Higher magnification of the area with plenty of mucin-secreting glands. Immunoreactive CD31 label the surface of endothelial cells, but not mucin of the tumour.

monia was observed in four patients with lesions of the central type, and distal bronchial dilation and mucoid impaction was seen in all five cases. The secondary findings associated with bronchial stenosis or obstruction on the HRCT scans largely reflected these pathologic findings. No lymph node metastasis was found in any of the surgical specimens.

4. Discussion

Mucoepidermoid carcinoma of the lung was first reported by Smetana et al. [11], and accounts for only a very small proportion of primary lung cancers. The tumours are classified as low grade or high grade based on their histologic appearance, and grading is based on cellular atypia, mitotic activity, local extension and tumour necrosis. Low-grade mucoepidermoid carcinoma is the most common type, and all five of the tumours in our series were low-grade. Although there is good clinicopathological evidence for the existence of the low-grade type, it has been questioned whether the high-grade type is a separate entity, mainly because of its histological similarity to mixed pulmonary carcinomas [5]. The high-grade variant is occasionally difficult to differentiate from adenosquamous carcinoma [12–14].

The most common symptoms are related to intraluminal growth, and these include persistent cough and sputum, wheezing, dyspnea, recurrent pneumonia, and, less frequently, hemoptysis [15]. Since the symptoms do not differ from those of other forms of lung tumour, they do not contribute to the differential diagnosis. Most patients with mucoepidermoid carcinoma are misdiagnosed as having bronchitis or lung carcinomas of other types. In our series, one patient was asymptomatic and the others had such similar symptoms that they were initially misdiagnosed as having chronic obstructive airway disease or other airway tumours.

Although the central-type tumours in our series were readily visible, only two of them were diagnosed preoperatively as mucoepidermoid carcinoma. Since mucoepidermoid carcinomas of the bronchi are usually covered by normal respiratory mucosa, bronchial brushing and lavage are seldom diagnostic, and it is better to perform a biopsy with forceps. Despite the theoretical risk of severe hemorrhage by performing a biopsy on a vascular mass, hemorrhage has never been reported as a complication of biopsy for mucoepidermoid carcinoma of the bronchus. Nevertheless, care is required because of the highly vascular nature of many of the tumours.

CT scan is non-invasive and useful for evaluating suspected endobronchial lesions, and fine morphological features have been revealed since the introduction of HRCT. In this series, HRCT images were essential for identifying the more detailed characteristics of the tumours, such as the margin, shape, density and pattern of enhancement. For the most part, the HRCT images reflected the pathologic features of the tumours well. There have been a few case reports of the HRCT appearance of mucoepidermoid carcinoma of the lung [7,10]. The HRCT features of the tumours in our series, such as a smooth margin and a well defined oval or round shape, were similar to those reported by Kim et al., who also found intratumoral punctate calcification on non-enhanced CT scans. Secondary findings associated with bronchial stenosis or obstruction, such as distal obstructive pneumonia, bronchial dilatation and atelectasis, were also seen. Although in their series Kim et al. reported mucoepidermoid carcinoma of the bronchus as showing mild contrast enhancement on CT scans, the three lesions of the central type and one lesion of the peripheral type in our series demonstrated marked contrast enhancement on HRCT images. The attenuation coefficients of the markedly enhanced tumours were much higher than those of the chest wall musculature.

Immunohistochemical staining for CD31 highlighted the heterogeneous distribution of blood vessels from mucin-secreting areas to non-secreting areas in a single tumour. In other words, these lesions may have characteristics of both hypervascular and hypovascular components, and the presence of both was probably the explanation for the features we observed on HRCT. The results of this study suggested that the presence of abundant microvessels, detected immunohistochemically by microscopic examination, affected the enhancement pattern on HRCT. These histopathologic findings correlated with the HRCT findings in all patients.

Bronchogenic carcinomas with more common histologic features, including adenocarcinoma, squamous cell carcinoma and small cell carcinoma have a variety of radiologic manifestations. Adenocarcinoma is often distinct from the other histologic subtypes of lung cancer. Non-solid nodules (ground glass opacities) and partly solid nodules (mixed solid/ground glass opacities) are recognized patterns of adenocarcinoma. Henschke et al. reported that the malignancies in subsolid nodules were typically bronchioloalveolar carcinomas or adenocarcinomas with bronchioloalveolar features, whereas in solid ones the malignancies were typically other subtypes of adenocarcinoma [16]. The proportion occupied by the non-solid component based on volumetric analysis by CT scan is a reliable predictor of tumours without vessel invasion in patients with adenocarcinoma of the lung [17]. Central squamous cell carcinoma is characterized by two major patterns of spread: intraepithelial spread with or without subepithelial invasion, and endobronchial polypoid growth. Polypoid tumours often occlude the bronchial lumen, resulting in atelectasis and obstructive pneumonia. Peripheral squamous cell carcinomas are seen as solid nodules, occasionally with cavitation and irregular margins. Approximately 90–95% of all small cell lung cancers are located centrally and show mediastinal or hilar lymphadenopathy with displacement or narrowing of the tracheobronchial tree or major vessels [18]. These common histologic types of lung cancer usually show mild or less contrast enhancement on CT images. Since these CT findings in common forms of lung carcinoma differ from those of mucoepidermoid carcinoma, which are relatively characteristic, contrast-enhanced CT may be helpful for lesion characterization and tumour classification in affected patients. If a marked heterogeneous contrast enhancement pattern is observed in well circumscribed oval or round masses of the bronchus, mucoepidermoid carcinoma can be considered in the differential diagnosis.

Large cell neuroendocrine carcinoma shows non-specific CT findings similar to those of other non-small cell lung cancer. On contrast-enhanced CT scans, tumour attenuation varies from slightly less to more than that of the chest wall muscle, with a homogeneous or heterogeneous pattern [18,19]. However, large cell neuroendocrine carcinoma is more likely to appear in the peripheral lung. Adenosquamous carcinoma of the peripheral type also usually shows heterogeneous soft-tissue attenuation [20]. Histopathologically, adenosquamous carcinoma is occasionally difficult to differentiate from high-grade mucoepidermoid carcinoma, which invades the pulmonary parenchyma in nearly 46% of the cases [3,12–14].

Pulmonary carcinoid tumours, which are low-grade malignancies accounting for 2–3% of all lung neoplasms [21], show CT findings similar to those of mucoepidermoid carcinoma. Pulmonary carcinoid tumours are also known to be vascular, and often show marked contrast enhancement on CT images [18,22]. Therefore, it is difficult to differentiate pulmonary carcinoid tumour from mucoepidermoid carcinoma on the basis of the CT contrast enhancement pattern alone.

Follow-up information was available for all five of the present cases. The clinical course of the patients was correlated with the histologic grade of their tumours. Low-grade mucoepidermoid carcinoma generally grows locally and is amenable to complete surgical resection. Low-grade tumours spread to regional lymph nodes by local growth in less than 5% of cases, and distant spread is rare [3,15]. The prognosis of low-grade tumours is usually excellent, with no evidence of local recurrence or metastasis. However, Barsky et al. [23] reported cases that were diagnosed as well differentiated and low-grade malignancy histologically but were rated as high-grade malignancy clinically. It can therefore be concluded that the histologic malignancy level of the tumour is not always the same as its clinical malignancy level. This suggests that complete surgical resection plus lymph node dissection should be performed for low-grade mucoepidermoid carcinoma of the bronchus as well as high-grade mucoepidermoid carcinoma. All five patients in our series underwent lobectomy plus lymph node dissection or sampling, and all are currently alive without evidence of disease at an average of 50.4 months after surgery (range, 15–82 months; median, 57 months).

5. Conclusions

We reviewed the HRCT and pathologic findings in five cases of mucoepidermoid carcinoma of the lung. Mucoepidermoid carcinoma is often visualized as marked heterogeneous contrast enhancement on HRCT images. The presence of abundant microvessels, detected immunohistochemically by microscopic examination, may affect the enhancement pattern on HRCT. However, examinations of HRCT images of mucoepidermoid carcinoma of the lung are insufficient because of the rarity of the tumour. The HRCT characteristics of the tumour must therefore be evaluated in more cases.

Conflict of interest

None declared.

References

[1] Colby TV, Koss MN, Travis WD. Tumors of salivary gland type. Tumors of the lower respiratory tract: AFIP atlas of tumor pathology 3rd series, vol. 13. Washington, DC: American Registry of Pathology; 1995. p. 65–89.
[2] Spencer H. Bronchial mucous gland tumours. Virchows Arch A Pathol Pathol Anat 1979;383:101–15.
[3] Yousem SA, Hochholzer L. Mucoepidermoid tumors of the lung. Cancer 1987;60:1346–52.
[4] Miller DL, Allen MS. Rare pulmonary neoplasms. Mayo Clin Proc 1993;68:492–8.
[5] Klacsmann PG, Olson JL, Eggleston JC. Mucoepidermoid carcinoma of the bronchus: an electron microscopic study of the low grade and the high grade variants. Cancer 1979;43:1720–33.
[6] Heitmiller RF, Mathisen DJ, Ferry JA, Mark EJ, Grillo HC. Mucoepidermoid lung tumors. Ann Thorac Surg 1989;47:394–9.
[7] Kim TS, Lee KS, Han J, Im JG, Seo JB, Kim JS, et al. Mucoepidermoid carcinoma of the tracheo-bronchial tree: radiographic and CT findings in 12 patients. Radiology 1999;212:643–8.
[8] Fisher DA, Mond DJ, Fuchs A, Khan A. Mucoepidermoid tumor of the lung: CT appearance. Comput Med Imaging Graph 1995;19:339–42.

[9] Tsuchiya H, Nagashima K, Ohashi S, Takase Y. Childhood bronchial mucoepidermoid tumors. J Pediatr Surg 1997;32:106–9.
[10] Kinoshita H, Shimotake T, Furukawa T, Deguchi E, Iwai N. Mucoepidermal carcinoma of the lung detected by positron emission tomography in a 5-year-old girl. J Pediatr Surg 2005;40:E1–3.
[11] Smetana HF, Iverson L, Swan LL. Bronchogenic carcinoma. Analysis of 100 autopsy cases. Milit Surg 1952;3:335–51.
[12] Leonardi HK, Jung-Legg Y, Legg MA, Neptune WB. Tracheobronchial mucoepidermoid carcinoma: clinicopathological features and results of treatment. J Thorac Cardiovasc Surg 1978;76:431–8.
[13] Stafford JR, Pollock J, Wenzel BC. Oncocytic mucoepidermoid tumor of the bronchus. Cancer 1984;54:94–9.
[14] Stafford JR, Pollock J, Wenzel BC. Bronchial mucoepidermoid carcinoma metastatic to skin. Report of a case and review of the literature. Cancer 1986;58:2556–9.
[15] Granata C, Battistini E, Toma P, Balducci T, Mattioli G, Fregonese B, et al. Mucoepidermoid carcinoma of the bronchus. Paediatr Pulmonol 1997;23:226–32.
[16] Henschke CI, Yankelevitz DF, Mirtcheva R, McGuinness G, McCauley D, Miettinen OS, et al. CT screening for lung cancer: frequency and significance of part-solid and nonsolid nodules. AJR Am J Roentgenol 2002;178:1053–7.
[17] Tateishi U, Uno H, Yonemori K, Satake M, Takeuchi M, Arai Y. Prediction of lung adenocarcinoma without vessel invasion: a CT scan volumetric analysis. Chest 2005;128:3276–83.
[18] Chong S, Lee KS, Chung MJ, Han J, Kwon OJ, Kim TS. Neuroendocrine tumors of the lung: clinical, pathologic, and imaging findings. Radiographics 2006;26:41–57.
[19] Oshiro Y, Kusumoto M, Matsuno Y, Asamura H, Tsuchiya R, Terasaki H, et al. CT findings of surgically resected large cell neuroendocrine carcinoma of the lung in 38 patients. AJR Am J Roentgenol 2004;182:87–91.
[20] Yu JQ, Yang ZG, Austin JH, Guo YK, Zhang SF. Adenosquamous carcinoma of the lung: CT-pathological correlation. Clin Radiol 2005;60:364–9.
[21] Davila DG, Dunn WF, Tazelaar HD, Pairolero PC. Bronchial carcinoid tumors. Mayo Clin Proc 1993;68:795–803.
[22] Fauroux B, Aynie V, Larroquet M, Boccon-Gibod L, Ducou le Pointe H, Tamalet A, et al. Carcinoid and mucoepidermoid bronchial tumours in children. Eur J Pediatr 2005;164:748–52.
[23] Barsky SH, Martin SE, Matthews M, Gazdar A, Costa JC. "Low grade" mucoepidermoid carcinoma of the bronchus with "high grade" biological behavior. Cancer 1983;51:1505–9.

The Impact of Residual Tumor Morphology on Prognosis, Recurrence, and Fistula Formation after Lung Cancer Resection

Takeshi Kawaguchi, MD, Shun-ichi Watanabe, MD, Riken Kawachi, MD, Kenji Suzuki, MD, and Hisao Asamura, MD

Introduction: The prognosis and proper management of patients with microscopic residual tumor at the bronchial resection margins (bronchial R1) remain unclear.

Methods: We performed a retrospective analysis of 74 patients who underwent pulmonary resection for lung cancer between 1976 and 2003 and had bronchial R1. The prognosis, pattern of the recurrence, and occurrence of the bronchopleural fistula (BPF) were analyzed according to the types of bronchial R1 morphology: direct extension (DIR, $n = 11$), peribronchial extension (PER, $n = 54$), and carcinoma in situ (CIS, $n = 9$).

Results: Five-year survival rates of patients with DIR, PER, and CIS were 0, 10, and 63%, respectively. The patients with CIS showed significantly better prognosis than those with DIR and PER ($p = 0.0006$, $p = 0.0009$, respectively). No prognostic difference was observed between patients with DIR and PER ($p = 0.1753$). Recurrent disease developed in 43 patients (58%). Only one of nine patients with CIS (11%) had recurrence, whereas 6 of 11 patients with DIR (55%) and 36 of 54 patients with PER (67%) had disease relapse. The recurrence rate in the CIS group was significantly lower than those of the other two groups (CIS versus DIR, $p = 0.036$; CIS versus PER, $p = 0.006$, respectively). BPF formation was not detected in patients with CIS; however, BPF developed in 3 of 11 patients with DIR (27%) and 3 of 54 patients with PER (5.6%).

Conclusions: Residual tumor morphology influenced the prognosis of patients with postresection bronchial R1 disease.

Key Words: Non-small cell lung cancer, Lung resection, Bronchial R1, Bronchopleural fistula.

(*J Thorac Oncol.* 2008;3: 599–603)

Surgical resection is the only potentially curative treatment for non-small cell lung cancer. A gross incomplete resection is associated with poor prognosis and high local recurrence and surgical complication rates.[1–3] Nevertheless, several reports have suggested that microscopic residual disease at the bronchial margin (bronchial R1, according to the tumor, node, metastasis classification of the International Union Against Cancer[4]) does not have the adverse effect on survival that gross residual disease does.[5–12] The prognosis and optimal postoperative management for patients with bronchial R1 disease remain unclear.

To clarify the prognosis, pattern of recurrence, and rate of bronchopleural fistula (BPF) formation in patients with R1 disease, we retrospectively reviewed the records of lung cancer patients who had been treated with pulmonary resection at our hospital, focusing on the relationship between R1 morphology and outcomes.

PATIENTS AND METHODS

Patients

Between June 1976 and June 2003, 4493 patients underwent pulmonary resection for primary lung cancer at the National Cancer Center Hospital, Tokyo. We included all patients ($n = 74$; 1.6%) who received at least lobectomy with mediastinal lymph node dissection and had microscopic residual tumor at the resected end of the bronchus in our retrospective analysis. Histologic typing and disease stage were classified according to World Health Organization classification[13] and tumor, node, metastasis classification of the International Union Against Cancer,[4] respectively. We excluded patients with small cell lung cancer or low-grade malignant histologic types, such as carcinoid or adenoidcystic carcinoma, from this study. Patient characteristics are shown in Table 1. Patients included in this study tended to have advanced (stages III and IV) disease and squamous cell histology.

Intraoperative frozen section examination of the bronchial margins was performed for 28 patients (38%). Although 26 of 28 patients had positive margins detected during surgery they did not undergo further resection because of limited pulmonary reserves or poor risk. Intraoperative examination found the bronchial margins to be tumor-free for two patients, however, postoperative analysis revealed bronchial R1 disease. Forty-six patients did not undergo intraoperative microscopic analysis of the bronchial stump because the bronchial resection line was considered tumor-free according to macroscopic examination.

Division of Thoracic Surgery, National Cancer Center Hospital, Chuo-ku, Tokyo, Japan.

Disclosure: The authors declare no conflict of interest.

Address for correspondence: Hisao Asamura, MD, Division of Thoracic Surgery, National Cancer Center Hospital, 1-1 Tsukiji 5-chome, Chuo-ku, Tokyo 104-0045, Japan. E-mail: hasamura@ncc.go.jp

ISSN: 1556-0864/08/0306-0599